Micro Total Analysis Systems 2004

Proceedings of μTAS 2004
8th International Conference on Miniaturized Systems
in Chemistry and Life Sciences
September 26-30, Malmö, Sweden

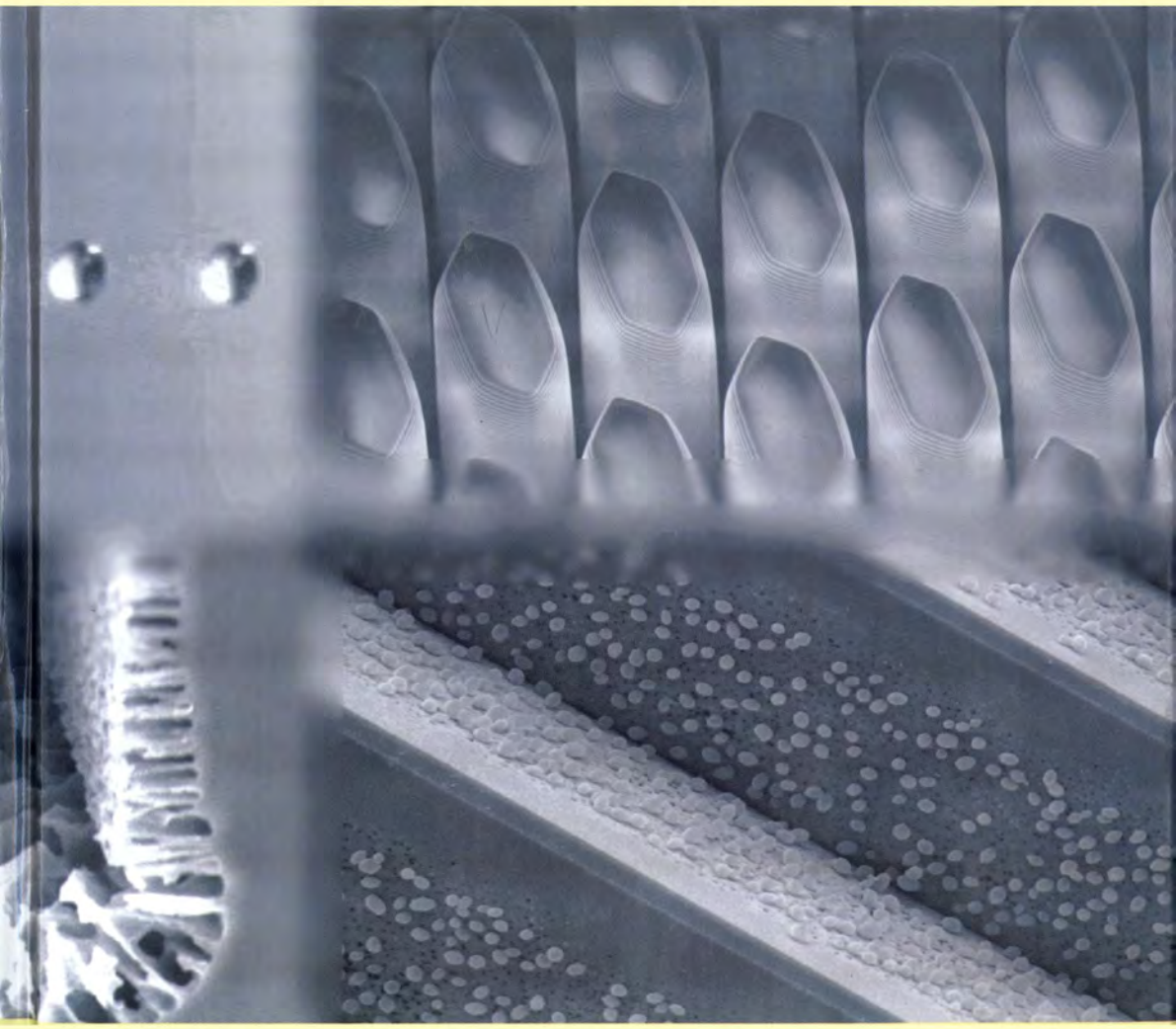

**EDITORS: Thomas Laurell, Johan Nilsson,
Klavs Jensen, D. Jed Harrison and Jörg P. Kutter**

Micro Total Analysis Systems 2004

Micro Total Analysis Systems 2004
Volume 2

Proceedings of μTAS 2004
8th International Conference on Miniaturized Systems for Chemistry and Life Sciences

Malmö, Sweden
September 26-30, 2004

edited by

Thomas Laurell
Lund Institute of Technology, Sweden

Johan Nilsson
Lund Institute of Technology, Sweden

Klavs Jensen
Massachusetts Institute of Technology, USA

D. Jed Harrison
University of Alberta, Canada

Jörg P. Kutter
Technical University of Denmark, Denmark

RS•C
advancing the chemical sciences

Special Publication No. 297

ISBN 0-85404-896-0

A catalogue record for this book is available from the British Library

Published by The Royal Society of Chemistry,
Thomas Graham House, Science Park, Milton Road,
Cambridge CB4 0WF, UK

Registered Charity Number 207890

For further information see our web site at www.rsc.org

Printed by Athenaeum Press Ltd, Gateshead, Tyne and Wear, UK

PREFACE

The 8th International Conference on Miniaturisation in Chemistry and Life Sciences, MicroTAS (Micro Total Analysis Systems) is celebrating its 10th anniversary year. The conference developed from a small gathering of researchers active in the field of MicroTAS in Enschede, The Netherlands, in 1994 with 160 participants. The success of this first meeting was followed by an equally appreciated μTAS workshop in Basel, Switzerland, in 1996 with a remarkable increase in the number of participants to 275. Optimism in the research field continued and the subsequent event was the truly unforgettable conference organised in Banff, Canada in 1998, with a record-breaking 420 conference delegates and about 130 papers submitted. At the following meeting in 2000, the conference returned to its birth place in Europe (at the University of Twente, Enschede, The Netherlands) again breaking new records for the MicroTAS conference with close to 500 attendees and about 140 scientific papers accepted (230 submissions). Due to the increasing interest that the MicroTAS/Lab-On-A-Chip field was generating, the subsequent meeting in 2001, in Monterey, CA, USA, forced the conference format into two parallel oral sessions in order to meet the pressure from the scientific community. In spite of the 9-11 terrorist attack and subsequent restrictions in international travelling, the conference attracted about 790 delegates and 276 accepted scientific contributions. The meeting was also characterised by an impressive commercial exhibition, demonstrating the transition of several of the earlier μTAS developments into the industrial sector. The subsequent conference (2002) in Japan is forever etched into our minds both with respect to the excellent organisation and scientific programme as well as the wonderful setting in ancient Nara. Although difficulties were developing in the industrial and financial sectors, following the IT-crash, the Nara meeting attracted 710 delegates with 316 accepted scientific contributions. The next μTAS conference was organised in another glorious location, Squaw Valley, CA, USA, in October 2003 and despite the setback in the global economy which clearly also affected academic budgets the conference attracted over 650 delegates with 325 accepted scientific presentations.

This year's conference confirms the continuing increase in interest in the μTAS-research field. More papers were submitted than ever before, 657, giving the Technical Programme Committee a difficult task in the abstract evaluation procedure. Again the scientific programme expanded, now to encompass a total of 422 accepted scientific contributions. We also see a continuing strong presence from the industrial area with some new players, indicating a recovery in the financial sector.

These two volumes contain the proceedings of the MicroTAS 2004 conference in Malmö, Sweden, September 26-30. Every paper presented will also be made available from the Royal Society of Chemistry, Lab on a Chip web-site at www.rsc.org/loc. The proceedings from the μTAS 2003 conference can also be accessed from this site.

The content of this year's MicroTAS conference clearly shows that the efforts in developing cell-based microsystems are increasing. Not only is work quite frequently focused on cell manipulation, and on-chip culturing but also on complete microsystems

for cell transport, culturing, analysis and monitoring including feed-back systems are now presented. The transition to polymer-based technologies continues and the now widely used SU-8/PDMS platform has opened up the μTAS-field to all those who do not necessarily have access to high performance clean-rooms, which vastly broadens the number of players that can now access and work in the field. A clear trend is also the increase in microfluidic two-phase systems, which seems to have come to a point where the two-phase fluid handling is well controlled and, *e.g.,* applications with compartmentalised chemistry in oil-immersed aqueous droplets in streaming microsystems are seen. The more mature areas of chip-based separation science are still very strong moving towards applications in genomics, proteomics and diagnostics. An exciting development is the continued progress in nanotechnology and the study of microfluidic transport, and molecular interaction and separation in nanoscale channels, this year displaying a representation equal to those in cell-based microsystems.

Looking back at μTAS conferences over the last ten years I can conclude that the field has matured and broadened from the original very strong focus on chip-based capillary electrophoresis systems to encompass a new science field of an extremely interdisciplinary nature with materials physicists and analytical chemists at one end and cell & molecular biologists and clinicians at the other. The field of microfluidics with all its aspects in combination with micro- and nanotechnology and life science research is accelerating, finding new areas where the miniaturised scale really makes a difference, and this is, of course, what research in this area is all about! We can confidently look forward to another ten years of exciting developments in this scientific field.

Finally, I would like to express my thanks to all of those who helped in organising this conference. The local organising committee for their broad network to industrial supporters and exhibitors and for all the work that is not seen but is yet so necessary. The Technical Programme Committee for the seemingly endless work reading and evaluating the 650 submitted abstracts in a medieval castle in southern Sweden. This is a task on which the whole foundation of the MicroTAS conference rests. Malmö Conference Agency is greatly acknowledged and I would especially like to thank, Lars Nilsson, Anna Martinsson and Niklas Swedenborg for their excellent and hard work in making all the necessary practical arrangements come to fruition. I would like to express my deepest gratitude to Johan Nilsson and Jörg Kutter, without whom, the administration would have been a total disaster, and for their expedient and fluent processing of all protocols and endless abstract and proceedings databases.

Last but not least, I thank all of you in the μTAS-science community for compiling and contributing your cutting-edge research for these two proceeding volumes. Without you there would be no meeting!

Thomas Laurell
μTAS 2004 Chairman
July 14, 2004

Programme Committee

Thomas Laurell
(Conference Chairman)
Lund University

Jörg P. Kutter
(Conference Co-chairman)
Technical University of Denmark

Yoshinobu Baba
University of Tokushima

David Beebe
University of Wisconsin - Madison

D. Jed Harrison
University of Alberta

Klavs Jensen
Massachusetts Institute of Technology

Takehiko Kitamori
University of Tokyo

Johan Nilsson
Lund University

M. Allen Northrup
Microfluidic Systems Inc.

Shuichi Shoji
Waseda University

J. Michael Ramsey
University of North Carolina

Sabeth Verpoorte
University of Groningen

Jean Louis Viovy
Curie Institute

The Programme Committee and The Local Organising Committee kindly acknowledge the support from the following:

Gold sponsors

VINNOVA

The Crafoord Foundation

SCIENCE • MEDICINE • TECHNOLOGY

Swedish Foundation for Strategic Research

MCPT

micralyne

Silver sponsors

SAMSUNG

microplast ab®
www.microplast.se

GYROS

LUND UNIVERSITY

ATS MEDICAL

Bronze sponsors

silex MICROSYSTEMS

Johnson&Johnson

Caliper LifeSciences

mfsi MICROFLUIDIC SYSTEMS, INC.

Other support

analytical chemistry

Science AAAS

LAB ON A CHIP

www.rsc.org/loc

JOURNAL OF SEPARATION SCIENCE


PROTEOMICS


Nanotechnology
.net
The world of nanotechnology


Lab-on-a-Chip
.com


ELECTROPHORESIS

Table of Contents
Volume 2

Day 2 – Tuesday, September 28, 2004

Tuesday Poster Session – MEMS Technology I

Tuesday Poster Session – Materials

Tuesday Session A – Pumping

Tuesday Session B – Protein Crystallization

Day 3 – Wednesday, September 29, 2004

Plenary V

Wednesday Session A – Cell Lysis

Wednesday Session B – Separation

Wednesday Session A – Gene Analysis

Wednesday Session B – NMR

Wednesday Plenary VI

Wednesday Poster Session – Applications III

Wednesday Poster Session – MEMS Technology II

Wednesday Poster Session – Detection Techniques

Wednesday Session A – Two-Phase Systems

Wednesday Session B – Coupling to MS

Day 4 – Thursday, September 30, 2004

Thursday Session A – Cell Culture II

Thursday Session B – Analysis

Thursday Session A – Microfluidics, Others

Thursday Session B – On-Chip Monitoring

FABRICATING A THREE-DIMENSIONAL CHANNEL FOR MICRO-FLUIDIC DEVICES BY LASER ABLATION

Yoshikazu Yoshida[1], Tsutomu Neichi[1], Retsu Tahara[1], Jun Yamada[1], Hiroyuki Yamada[2] and Nobuyuki Terada[3]

[1]Toyo University, 2100 Kujirai, Kawagoe, Saitama 350-8585, Japan
[2]Yamanashi Pref. Industrial Technology Center, 2094 Kofu, Yamanashi 400-0055, Japan
[3]University of Yamanashi, 1110 Tamaho, Nakakoma, Yamanashi 409-3898, Japan

Abstract

This paper describes the fabrication in resin of micro-channels for micro-fluidic devices such as the μTAS (Micro Total Analysis System) by UV laser ablation process. A number of heat-hardening resin-films are layered on a soda glass. A laser fabricates a part of the channel on each film for every lamination. Then three-dimensional (3-D) confluence channels are fabricated. The fabricated channels are 45-180 μm in depth and 50-300 μm in width. The through holes are made in the laminate film with a laser. An inlet pipe for a micro-pump is inserted into the hole.

Keywords: μTAS, UV laser, lamination, resin-films, blood

1. Introduction

Recently, in various fields the necessity for small and highly sensitive micro-fluidic analysis systems has increase. Therefore a μTAS has received considerable attention. The μTAS is the size of a card, and has miniaturized channels, detectors, and other elements for fluidic analysis. The advantages of this system are the reduced need of fluidic samples, reagents, and hours of detection. The size of the fluidic analysis elements on the μTAS is a few score micrometers. There are many fabrication methods of micro-channels through semiconductor technology [1], plastic molding [2], and laser fabrication of resins [3]. The laser fabrication method has recently been receiving much attention. The advantages of this method are: one stroke fabrication of grooves for channels, an easy change of groove patterns, and 3-D fabrication to allow grooves with slopes and differences in levels. We have been proposing the method which uses silicon or quartz as the substrate part of μTAS, build the micro working parts and electrode in advance onto the substrate, then create the flow path and cistern on the resin part formed on the substrate [4]. An ultraviolet pulse laser was used to form such items as the flow path. A number of heat-hardening resin-films were layered on a soda glass. A laser fabricated a part of the channel on each film for every lamination, and then a 3-D micro-channel structure was fabricated. Two types of flow path, a plane and an overpass, are fabricated.

2. Experiment equipment

The substrate is soda glass laminated by heat-hardening resin-film. This film is made of two films, one of 25μm thick polyimide and the other 20μm thick epoxy. Channels are fabricated by a pulse Nd:YAG laser system (Brilliant; Quantel) and a KrF excimer laser system (LPX220; Lambda Physik, AG). For the experiment condition, the YAG has a wavelength of 266nm, pulse energy of 3.1mJ, pulse width of 4.3nsec, and repetition rate of 10Hz. The laser beam is fixed, and the substrate is moved in the XY stage. This stage has a positional bi-directional repeatability of ±5μm. The excimer has a wavelength of 248nm, output energy of 8-80W, maximum pulse energy of 450mJ, pulse width of 10-20nsec, and repetition rate of 25-200Hz. A mask is used to shape the laser beam into a square shape to allow fabrication with smooth wall surfaces at low overlap rate conditions. The laser beam is focused to the width of a groove.

3. Results and discussion

3.1 Three-pronged channel

Combining of laminar flows in a micro-channel makes possible the study of blood cell analysis. Figure 1 shows an optical photomicrograph of three-pronged grooves without cover film fabricated by the excimer laser. Channels have a width of 50μm and a depth of 45μm in three-pronged parts, and a width of 150μm in a confluence part. Blood is injected at a low flow rate between two rapidly flowing streams of physiological salt solution. The width of the stream of blood can be controlled by the height difference between a blood reservoir and solution reservoir, that is potential energy. The width narrows as it climbs to the speed of the neighboring streams. The width decreases with the increasing height difference. The cells velocity increases with the increasing height difference. In this experiment, the channel substrate is placed horizontally on a microscope stand, and the reservoir made from a connector between a syringe and a needle is connected to the channel inlet with Silicon tube. This tube has an external diameter of 1mm and an inside diameter of 0.3mm. Figure 2 shows a focused picture of blood when the blood reservoir is 200mm high and the solution is 400mm high from the channel. The cells velocity is almost 15.5mm/s. It is almost 9mm/s when the height difference is nearly zero. As shown in Fig.2 (b), blood cells can be measured individually.

3.2 Three-dimensional channels

Figure 3 shows the optical photomicrograph of a channel made on the second film by the YAG laser. The laser scanning distance is 150μm. The second film is peeled off from the first one by the scanning. The film placed between the scanning is removed from the substrate. The space caused by removal of the film is used as a channel space. The film peelings on the channel side are removed with the following laminating process.

Figure 4 shows the production process of the steric mixture flow path used to branch. There are 3-D pattern diagrams and optical photomicrographs each time a lamination is done. First, the channel element of the first layer is made for the film on the glass by the laser (Fig.4 (a)). After that, the second film is laminated on the first one, and the channel element is made on the film (b). These processes are iterated several times, and the 3-D confluence channel is fabricated. The channel is closed because the groove is treated with laminate processing, and liquid can't enter into the groove. Therefore it is necessary to make a perforated hole in the flow path to insert liquid inside, and connect the tube. The diameter of the hole is 150μm, and formed on the laminate film by laser drilling. Deionized water is injected into the channels with a microinjection pump. The flow rate is 5μL/min. There is no damage to the channel.

4. Conclusions

(1) The groove with a width from several dozen μm to several hundred μm is created on the resin layer without any damage on the substrate by ablation processing with an ultraviolet laser.
(2) A heat-hardening resin film can be used to maintain 100% of the channel space for fluid flow.
(3) Fresh blood flows easily through the channels.

References

[1] A.Manz et al., *J.Chromatography*, **593**, pp.253-258 (1992).
[2] N.Kitamura, H.B.Kim, and K.Ueno, *T.IEE Japan*, **121-E**, pp.169-174 (2001).
[3] F.Wagner and P.Hoffmann, *Proc.SPIE*, **4088**, pp.337-340 (2000).
[4] Y.Yoshida, *Proc.SPIE*, **5063**, pp.189-192 (2003).

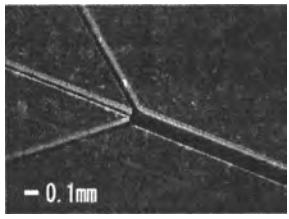

Figure 1. Side view micrograph of three-pronged grooves without cover film.

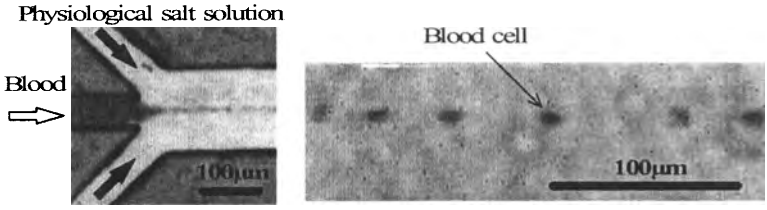

Figure 2. Blood pass-through in a three-pronged channel. The right photo shows the downstream.

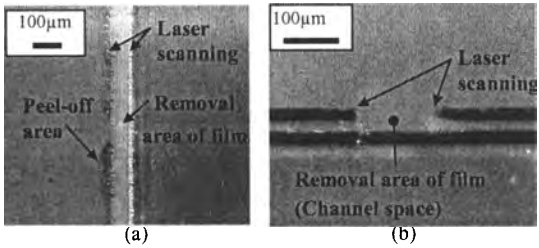

Figure 3. Micrograph of channels. (a)Top, and (b) cross-section.

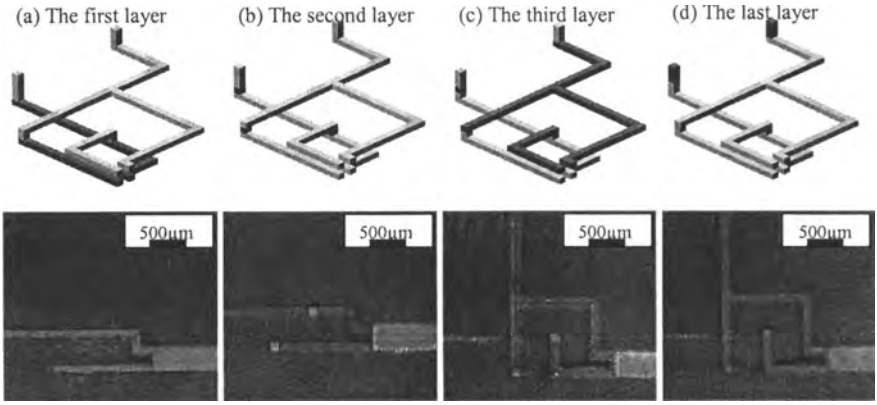

Figure 4. Fabrication process of 3-D channel image and photo of branch steric path.

PHOTOPOLYMERIZED POLY(ETHYLENE) GLYCOL DIACRYLATE (PEGDA) MICROFLUIDIC DEVICES

Amy Butterworth, Maria del Carmen Lopez Garcia and David Beebe
Department of Biomedical Engineering, University of Wisconsin
1550 Engineering Drive, 53704 Madison WI, USA

Abstract

As microfluidic applications in cell biology move beyond diagnostic assays to long term culture and production, alternative materials will be needed. Poly (ethylene) glycol (PEG) has been widely utilized as a biocompatible polymer due to its hydrophilicity and non-fouling behavior. Diacrylated, PEG can be photopolymerized using the microfluidic tectonics platform (μFT) and provides a more biocompatible alternative to previous polymers used. The ability of this monomer to be polymerized and patterned into channels for micro-cell culture was evaluated. Also, the biocompatibility of the polymer was assessed using FT-IR and cell interaction studies with the unpolymerized components.

Keywords: Microfluidic tectonics, biocompatibility, photopolymerization, poly (ethylene) glycol (PEG)

1. Introduction

Poly (ethylene) glycol (PEG) has been widely utilized as a biocompatible polymer due to its hydrophilicity and non-fouling behavior [1]. PEG resists protein absorption and has been used as a coating or as a polymer substrate to prevent or control cell adhesion and adsorption of proteins for over a decade. PEG has been used previously in bioMEMS-related technologies as a coating or as a co-monomer for purposes such as polymerizing cells in gels [2, 3]. Diacrylated, PEG can be photopolymerized using the microfluidic tectonics platform (μFT) [4] and provides a more biocompatible alternative to previous polymers used. The ability to incorporate PEG as a construction material for microfluidic systems will allow the unique properties of PEG to be exploited for a variety of cell-based experiments. Examples include using in-situ polymerized porous PEG gels as selective diffusional barriers to replace media changes during cell culture, or copolymerizing with a hydrolytically degradable monomer for controlled release of biomolecules of interest.

2. Fabrication and Biocompatibility Analysis

The biocompatibility of this polymer will be partially dependent on the complete polymerization of the monomer while using a minimal concentration of photoinitiator. The typical concentration of photoinitiator used in these experiments was 0.05 wt%, although lower percentages (below 0.01 wt%) can be polymerized but exhibit more swelling. To verify the degree of polymerization, FTIR studies were done, comparing the spectra of the polymer with 0.1 wt% photoinitiator (Fig. 1a) to that with 0.05 wt% (Fig. 1b). The polymerization of diacrylates reduces the magnitude of the carbon-carbon double bond peak (shown in Fig. 1) and is expected to decrease with increasing photoinitiator concentration as shown. FTIR measurements allow one to find a balance between concentration of photoinitiator and degree of polymerization that minimizes the cytotoxicity of the devices, while maintaining good patterning capabilities. After UV sterilization before use in cell culture, this peak decreased slightly. Straight channels were patterned to test the patterning capabilities, with widths ranging from 175μm to 1,000μm in 250 μm high devices (Fig. 2). Good resolution of less than 10μm was achieved which is comparable to that achieved with poly (IBA). A valve mask currently in use for creating the substrate for a hydrogel actuated valve

was also patterned in PEGdA with relative ease [5]. These two materials show similar capabilities although the PEGdA devices produce more rounded features.

Since our intended use of the PEG channels is long term (weeks) cell culture, the long term capability of the material was tested to ensure no failure occurred due to the PEGdA swelling. Swelling of the PEGdA material did cause device failure more frequently as the percentage of photoinitiator decreased (from 0.05 wt% to 0.01 wt%) and exposure intensities decreased (from 20 mW/cm^2 to 10 mW/cm^2). The molecular weight of the PEGdA was reduced from 575 MW to 258 MW, which showed significantly reduced swelling and produced devices which could be incubated at 37°C without immediate failure. Multiple photoinitiators 4-(2-hydroxyethoxy)phenyl-(2-hydroxy-2-propyl) ketone (Irgacure 2959, Ciba, Inc.) and biacylphosphine oxide (BAPO, Iragure 819, Ciba, Inc.) were also studied. The former has commonly been used for photopolymerization of cells in gels and has shown to be more biocompatible than many photoinitiators. The latter has a higher efficiency (the absorption band extends to 400nm) at the wavelengths of exposure, so lower concentrations were needed. Successful polymerization was demonstrated with both compounds, although BAPO-initiated devices proved to be more resistant to swelling most likely due to the faster reaction kinetics causing denser gels.

4. Biocompatibility

Devices were created with the optimized prepolymer mixtures and exposures with 1,000μm straight channels and incubated with DPBS at 37°C. When externally reinforced with adhesive, these devices are suitable for cell culture, surviving for more than one week without failure due to swelling of the polymer. The cellular response to the presence of the monomer and photoinitiator in the media was evaluated. A concentration of 10 μM PEGdA caused significant reduction in NMuMG cell adhesion, while 1μM did not prevent adhesion, although cell morphology was slightly different than the controls. Cells with PEGdA in the media that did attach to the surface remained rounded in colonies rather than spreading as expected for epithelial cells. Due to very low solubility of BAPO in the media, quantitative results were not obtained, although the presence of BAPO did cause cell death in media with the maximum soluble amount of BAPO. It is clear that further optimization of the polymerization technique and prepolymer mixture is needed to ensure minimal concentrations of prepolymer components remain after polymerization and washing in order to maximize biocompatibility.

References

[1] S. Sharma, K. C. Popat, and T. A. Desai, "Controlling nonspecific protein interactions in silicon biomicrosystems with nanostructured poly(ethylene glycol) films," *Langmuir*, **18**, 8728-8731 (2002).

[2] S. J. Bryant, C. R. Nuttelman, and K. S. Anseth, "Cytocompatibility of UV and visible light photoinitiating systems on cultured NIH/3T3 fibroblasts in vitro," *Journal of Biomaterials Science-Polymer Edition*, **11**, 439-457 (2000).

[3] Y. Hanein, Y. Vickie Pan, B. D. Ratner, D. D. Denton, and K. F. Bohringer, "Micromachining of non-fouling coatings for bio-MEMS applications," *Sensors and Actuators, B: Chemical*, **81**, 49-54 (2001).

[4] D. J. Beebe, J. S. Moore, Q. Yu, R. Liu, M. Kraft, B. Jo, and C. Devadoss, "Microfluidic tectonics: A comprehensive construction platform for microfluidic systems," *PNAS*, **97**, 13488-13493 (2000).

[5] D. Kim and D. Beebe, "In-Situ Fabricated Micro Check-Valve Utilizing the Spring Force of a Hydrogel," presented at Proceedings of the Micro Total Analysis Systems, Lake Tahoe, CA, USA (2003).

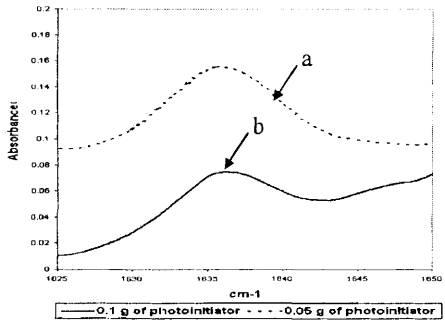

Figure 1. FTIR spectra of photopolymerized PEGdA, (a) with 0.1 wt% photoinitiator and (b) with 0.05 wt% photoinitiator. The amount of carbon-carbon double bonds decreases with increasing photoinitiator showing the increased polymerization of the PEGdA. A balance between concentration of photoinitiator and free monomer after polymerization will maximize biocompatibility.

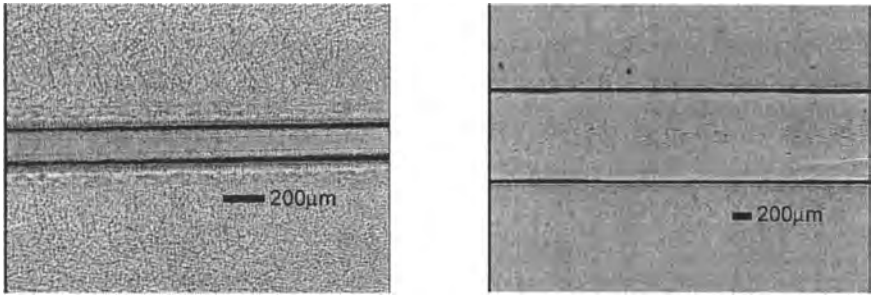

(a) (b)

Figure 2. Channel walls patterned in PEGdA, (a) 175µm width, and (b) 1,000µm width. An accuracy of less than 10µm was achieved with both channel widths.

A FLOW-THROUGH SHEAR-TYPE MICROFILTER CHIP FOR SEPARATING PLASMA and VIRUS PARTICLES FROM WHOLE BLOOD

Levent Yobas[1], Ee-Ling Gui [2], Hongmiao Ji[1], Jing Li[1], Yu Chen[1], Wing-Cheong Hui[1], Siti Rafeah Binte Mohamed Rafe[3], Sanjay Swarup[4], Sek-Man Wong[4], Tit-Meng Lim[4] Chew-Kiat Heng[3]

[1]Institute of Microelectronics, 11 Science Park Road, Singapore Science Park II, 117685, Singapore

[2]Nanyang Technological University, School of Materials Engineering, 639798, Singapore

[3]National University of Singapore, Department of Pediatrics, 119074, Singapore

[4]National University of Singapore, Department of Biological Sciences, 117543, Singapore

Abstract

A flow-through shear-type microfilter chip has been proposed for the purpose of separating plasma and virus particles from whole blood. The microfilter chips have been fabricated in three different design configurations by silicon micromachining and tested for their percent efficiency of separating plasma from diluted blood samples. One of the designs has been further demonstrated to be capable of isolating virus particles from a spiked sample of whole blood.

Keywords: Microfilter, shear filter, virus, plasma, sample preparation

1. Introduction

Recent epidemics such as Severe Acute Respiratory Syndrome (SARS) have highlighted the importance of an automated sample preparation for virus and pathogen detection. Detection of extracelullar viruses from blood usually requires separation of plasma or serum containing virus particles from cellular components. This is because hemoglobin from red blood cells (RBC) is known to inhibit nucleic acid amplification while nucleic acids in white blood cells (WBC) can contribute to background noise during detection [1]. Typically, plasma is obtained from whole blood by a centrifugation step. Nevertheless, centrifugation is not amenable to automation. An alternative approach is filtering plasma based on size exclusion of cells [2]. Most viruses are less than 1μm while most RBC and WBC remain larger than 2μm.

2. Microfilter Chip

The proposed microfilter concept and structure are diagrammatically shown in Fig. 1. The chip contains a chamber etched about 65-μm deep into silicon by deep reactive ion etching and capped with a glass wafer by anodic bonding. Plasma can be collected through anisotropically-etched backside holes in silicon located at two diagonal corners. At the other corners, backside holes allow blood to flow in and out of the chip through a meander type channel defined by silicon pillars. As blood flows inside the channel, plasma can escape through narrow slits between pillars due to combined action of capillary forces and pressure gradient. Nominal gap between the pillars is about 1.6μm wide, which can retain most blood cells but allow passage of virus particles. The microfilter chips have been fabricated in three design configurations mainly differing in chip size and shape of the meander-type channel (Table I).

3. Experimental Results & Discussion

Fig. 2 shows on-chip collection of plasma escaping through the slits between pillars as the anticoagulant-treated whole blood flows through the meander-type channel. Anticoagulant-treated blood was pumped through the chips at 10μl/min and at different dilutions of phosphate buffered saline (PBS) solution. RBC counts in the blood pumped in (RBC_{blood}) and the plasma collected

(RBC_{plasma}) were obtained by a hemocytometer. Table I shows volume of the collected plasma samples and percent efficiency of each microfilter chip (% EF) as calculated by:

$$EF = \left[1 - \left(RBC_{plasma} / RBC_{blood}\right)\right] \times 100 \quad (1)$$

As shown, chips based on any of the three designs had higher than 99% efficiency for the Blood:PBS ratio of 25:75. The efficiency deteriorated with an increase in the blood:PBS ratio but stayed above 90% for all three microfilter chips.

Further, experiments were conducted to test whether the plasma filtered by the microfilter chips can be used for detection of virus particles in blood. Anticoagulant-treated whole blood at a volume of 140μl was spiked with virus (Cymbidium Mosaic Virus) suspension in water at a volume of 70μl and concentration of 0.26μg/μl. Approximately, 180μl of the spiked blood was pumped through microfilter #1 at 10μl/min. The plasma filtrate was used for extraction of viral RNA via a commercial kit [3] and amplified by reverse transcription polymerase chain reaction (RT-PCR). The amplified products were separated by agarose gel electrophoresis and ethidium bromide-stained products were visualized on a UV transilluminator. As can be seen in Fig. 3, viral RNA from the plasma filtered by microfilter chip #1 could be amplified, demonstrating a successful substitute for the conventional centrifugation step.

References:

[1] McCusker J., et al. (1992) Nucleic Acids Res. 20, 6747

[2] Wilding, P., et al. (1998) Analytical Biochemistry, 257, 95-100.

[3] QIAamp® Viral RNA Mini Kit Handbook, 1999, Qiagen.

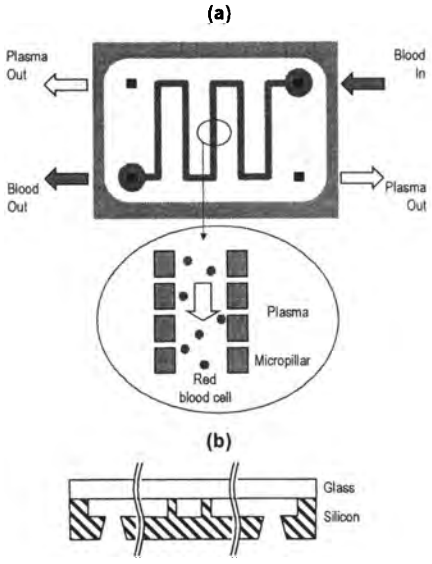

Figure 1: Diagram of the flow-through shear-type microfilter chip: (a) plane view with inset showing close-up of channel defined by pillars (b) cross section profile.

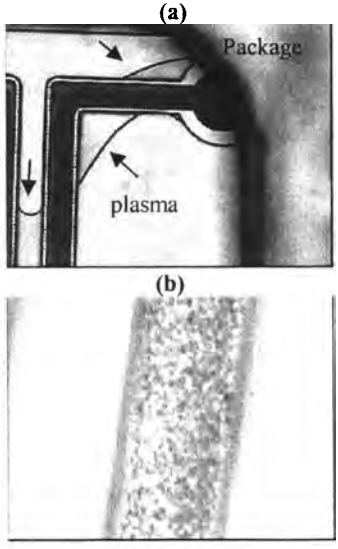

Figure 2: Plasma separation from whole blood (undiluted): (a) plasma escaping (arrows) through narrow slits between pillars (b) close-up view of red blood cells inside the channel.

Table 1: Microfilter chips characterization for two different ratios of Blood:PBS volume

Blood:PBS Volume ratio			50:50	25:75
RBC count in the blood pumped in (Million)			865	433
Volume of the diluted blood pumped in (µl)			400	400
Microfilter #1 (5mm by 10mm)		% EF	90.37	99.56
		Plasma collected (µl)	212	181
Microfilter #2 (5mm by 10mm)		% EF	95.08	99.47
		Plasma collected (µl)	224	139
Microfilter #3 (10mm by 10mm)		% EF	91.30	99.81
		Plasma collected (µl)	198	61

1: 8.46 x10^8 cp/µl
2: 4.23 x10^8 cp/µl
3: 2.12 x10^8 cp/µl
4: 1.05 x10^8 cp/µl
5: 5.30 x10^7 cp/µl
6: Centrifuge (dilution x100)
7: Centrifuge (dilution x10,000)
8: Negative
9: Microfilter #1(Dilution x10)
10: Microfilter #1 (Dilution x1,000)
M: Marker (100bp)

Figure 3: RT-PCR products of Cymbidium Mosaic Virus RNA separated by agarose gel electrophoresis: 1 to 5: dilution-series of standards, 6 and 7: plasma from spiked blood prepared by centrifuge, 9 and 10: plasma from spiked blood prepared by the microfilter # 1.

ULTRA-SMOOTH GLASS CHANNELS ALLOWING NON-FLUORESCENT OBSERVATION OF BIO-MOLECULES BY MICROSCOPES

Ryuji Yokokawa, Shoji Takeuchi, Hiroyuki Fujita
CIRMM/IIS, The University of Tokyo, 4-6-1, Komaba, Meguro, Tokyo 153-8505, Japan

Abstract

Optically flat glass channels were fabricated; in the channel two kinds of bioassays were successfully monitored. As result of assays microtubules and kinesin-coated beads were clearly observed by a dark-field microscope and a differential interference contrast (DIC) microscope, respectively. We have optimized the concentration of HF to obtain a flat surface and evaluated the surface by AFM, SEM, and the dark-field microscopy. The glass channel was etched using a poly(dimethyl siloxane) (PDMS) micro fluidic channel as an etching mask, and then sealed with a PDMS-coated coverslip permanently. The volume of the channel, 2-3 μl, realized the drastic reduction of the amount of protein required for an assay compared with a conventional flow cell method requiring 20 μl.

Keywords: glass etching, microfluidic channel, dark-field microscope, differential interference contrast microscope, protein

1. Introduction

Dark-field and DIC microscopy are major techniques to visualize raw proteins of nanometers in size without fluorescent labels. Biochemists have used a flow cell composed of two glass plates with spacers to enclose proteins between optically flat surfaces [1-2]. This technique, however, requires at least 20 μl of protein samples per assay, because the regular flow cell size is 10x18 mm^2 in area with 100 μm in height. The amount of a protein prepared by a purification process is limited to several hundreds of microliters. It is necessary to decrease the sample consumption in order to perform a time-effective analysis using limited samples. One approach is to utilize μTAS, but glass channels developed so far are not focused on the microscope observation [3-5].

Therefore we have fabricated microfluidic channels for that purpose. The ultra-smooth surface not only on the channel side but the lid surface is necessary, because even roughness or dirts of 10 nm in the optical axis cause the serious scattering of illumination light. We aimed to perform the bioassay including attachment of proteins on a glass surface and replacement of buffers in the sealed channel, so that we can reduce the assay time and the required amount of proteins at the same time.

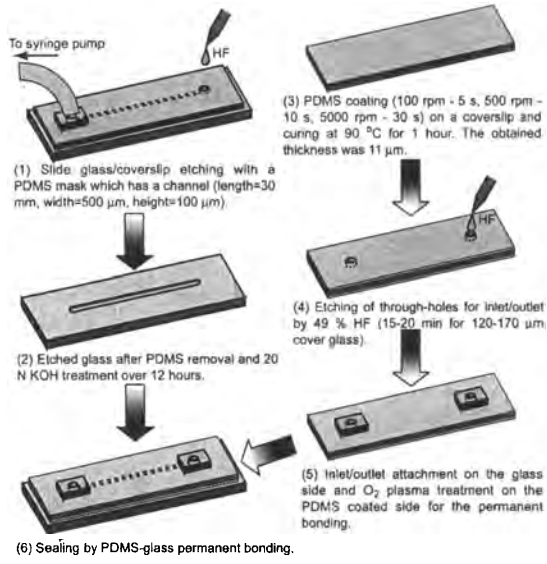

Figure 1. Fabrication process.

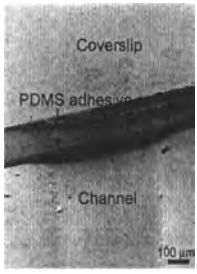

Figure 2. A sealed channel.

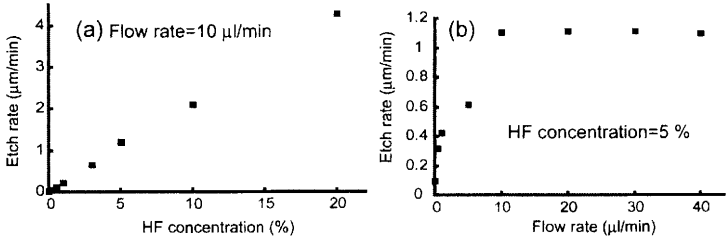

Figure 3. Etch rate vs. (a) HF concentration and (b) HF flow rate.

2. Experimental

Glass etching: A glass channel was directly etched on a slide glass (Matsunami) without annealing [5]. We utilized a PDMS mold as an etching mask, because PDMS is resistant to repetitive immersion of diluted HF [3]. The mask was first fabricated by pouring PDMS prepolymer to a mother mold patterned on a silicon wafer by DRIE. The cured PDMS replica (length=30 mm, width=500 μm, and height=100 μm) was just placed on a slide glass or a coverslip with slight pressure by hand to remove air bubbles (Fig. 1(1)). Only the channel region was etched by sucking the solution from the outlet with a syringe pump while supplying HF solution to the inlet as shown in Fig. 1(1, 2). The adhesion between PDMS and the glass surface was enough tight to prevent HF immersion during the etching process. Various concentrations of HF (0.01-20 %) was tested at various flow rates (0-40 μl/min).

Channel sealing: Channels were simply but permanently sealed with a PDMS-coated coverslip for the disposable use. A thin PDMS layer is an adhesion between an etched glass and a coverslip. PDMS prepolymer was coated by an optimized gradient spincoating (100 rpm - 5 s, 500 rpm - 10 s, 5000 rpm - 30 s) and cured at 90 °C for 1 hour. We obtained uniform thickness of 11 μm, although it was difficult to achieve a uniform layer with the viscous prepolymer (Fig. 1(3)). Through-holes for inlet and outlet were also etched by HF with a PDMS mask (Fig. 1-(4)). It was necessary to cover the whole glass surface by PDMS to protect it from etching by vaporized HF [6]. Inlet and outlet connectors were attached (Fig. 1(5)), and the coverslip was permanently bonded with the etched glass after O_2 plasma treatment (Fig. 1(6)). The etched channel, the PDMS layer for adhesion and the coverslip are shown in Fig. 2. The lid of coverslip with PDMS layer is partially broken to observe the cross section in Fig. 2. Some glass particles are also observed.

Assay test in the channel: Two kinds of bioassays, the bead assay and the gliding assays, were performed in a sealed channel and monitored. A well-known biomolecular motor, kinesin-microtubule system, was prepared for the assay. A motor molecule, kinesin (a few nanometers in size), moves on a rail molecule, microtubule (diameter=25 nm, length=10-30 μm), by hydrolyzing adenosine 5'-triphosphate (ATP). Proteins in buffer solutions were injected from the inlet and sucked from the outlet by the syringe pump. The required amount of solution for each injection was only 2 μl.

3. Results and discussion

Etching rate increased proportionally with the increase of HF concentration as shown in Fig. 3a. Flow rate of over 10 μl/min stabilized the etching rate (Fig. 3b) and also decrease the variation of etching depth along a channel. The average surface roughness (R_a) was measured over 20×20 μm^2 area by AFM (Fig. 4). R_a obtained from samples etched by 0.1-5 % HF are as good as R_a =0.96 from an original glass surface. But R_a drastically increases over 10 % HF. AFM images, however, show slight difference even between (a) the surface etched by 5 % HF and (b) the original glass

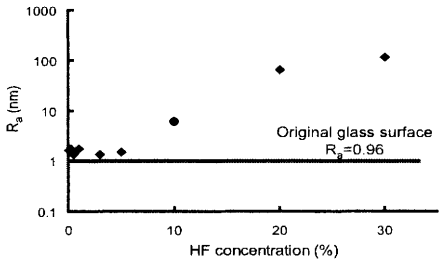

Figure 4. The relationship between surface roughness (R_a) and HF concentration.

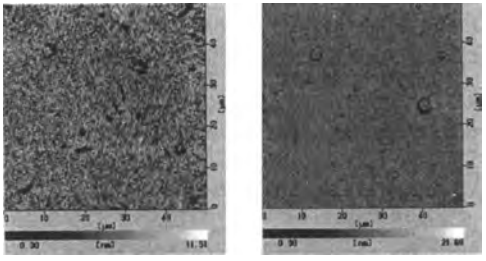

(a) 5 % HF (b) Original glass surface

Figure 5. AFM images of glass surfaces etched by different HF concentration. A scanned area is a 50 μm square.

surface as shown in Fig. 5; the former has higher density of etched pits than the latter. Since the roughness of less than 10 nm is achieved [3, 5], the scattered light from microtubule can be visualized under the dark-field microscope.

We have observed the kinesin-coated beads (320 nm in diameter) moving on immobilized microtubules on the etched surface using a DIC microscope (Fig. 6a). Each white dot corresponds to a bead and some larger dots are aggregated beads. We have also realized the gliding assay in which microtubules glide on the kinesin-coated etched glass surface. The movement of microtubules was visualized as white lines by the dark-field microscope as shown in Fig. 6b. Dirts contained in a buffer solution were also observed.

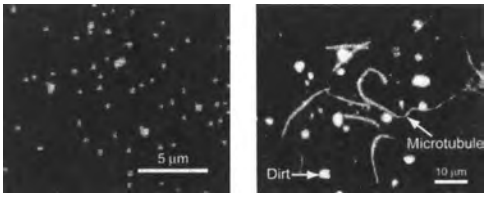

(a) Microbeads by DIC microscope (b) Microtubules by dark-field microscope

Figure 6. (a) kinesin-coated beads moving on microtubules and (b) microtubules gliding on the kinesin-coated glass surface.

4. Conclusion

The glass channel was fabricated with the ultra-smooth surface in the order of R_a=10 nm for bioassays. The optimized HF flow rate and the concentration during etching process were 10 μl/min and 5 %, respectively. A coverslip coated with a thin PDMS layer was utilized for the sealing of an etched glass channel. Finally, bioassays were performed to demonstrate the feasibility of channels, and nano-scale beads and microtubules were visualized. This proves the channel enables the observation of raw proteins with 1/10 sample volume of proteins compared with the conventional method.

Acknowledgements

Authors thank Prof. Kazuo Sutoh, Dr. Takahide Kon, and Mr. Masaya Nishiura at Graduate School of Arts and Sciences, The University of Tokyo for biological preparations.

References

[1] J. Howard *et al.*, Methods in cell biology, **39**, 137 (1993)
[2] H. Suzuki *et al.*, Jpn. J. Appl. Phys., **34**, 3937 (1995).
[3] I. Rodriguez *et al.*, Anal. Chim. Acta **496**, 205 (2003)
[4] A. Grosse *et al.*, J. Micromech. Microeng. **11**, 257 (2001)
[5] C-H Lin *et al.*, J. Micromech. Microeng. **11**, 726 (2001)
[6] Y. Fukuta *et al.*, Jpn. J. Appl. Phys., **42**, 3690 (2003)

DEVELOPMENT OF PERISTALTIC SOFT MICROPUMP DRIVEN BY ELECTROSTATIC ACTUATOR

Takaaki Suzuki[1], Isaku Kanno[1], Shunsuke Yakushiji[1],

Satoyuki Kawano[2] and Hidetoshi Kotera[1]

[1]Dept. of Mechanical Engineering, Kyoto University, Yoshida-Honmachi, Sakyo-ku, Kyoto 606-8501, Japan

[2]Center for Interdisciplinary Research, Tohoku University, Aramaki-aza Aoba, Aoba-ku, Sendai 980-8578, Japan

Abstract

We have developed a valveless micropump driven by electrostatic actuators. The micropump was composed of flexible wall of microchannel with electrodes for the electrostatic force. Traveling wave was induced on the surface of the microchannel by applying sinusoidal voltages to each electrode with the different phase. The fluid can be moved by the peristaltic motion of the channel wall. The sinusoidal voltages of 150 V were applied at the frequency of 5.0 kHz to the electrostatic actuators under the microchannel filled with the water. The fluid flow was measured with micro particle's motion in the fluid by the peristaltic actuation of electrostatic force.

Keywords: micropump, electrostatic, traveling wave

1. Introduction

A number of micropumps are proposed for fluid transportation system of μTAS. In most of conventional pumps, a diaphragm-type pumps which are actuated by piezoelectric actuators are popular because relatively large pumping power can be generated [1,2]. The fluid in the micropumps is transported by the vibration of diaphragm and the flow direction can be defined by mechanical valves. However, these micropumps have complicated structure, and therefore it is not easy to reduce the whole size of the pumps as well as the production cost. On the other hand, J. G. Smits reported a peristaltic micropump which realized a high flow rate of 100 μl/min [3]. This method enable simple structure and is suitable for the integration on a chip. We have also proposed a similar micropump system composed of a microchannel made of silicon rubber where the traveling wave is induced by PZT bimorph beams and demonstrated high efficiency of this type of micropump [4]. In this study, we adopted electrostatic actuators as a driving force of the micropump for practical application.

2. Experiment

Figure 1 shows the exploded illustration of the micropump. The microchannel is composed of PMMA with the height of 30 μm. Bottom surface of the microchannel is deformed by the electrostatic actuators whose upper electrodes are copper thin films deposited on a polyimide sheet. At the opposite side of the upper electrodes, lower electrodes were equipped with the gap of 7 μm. The lower electrodes, which were also deposited on the polyimide sheet, were separated to be actuated with the different phase. An overview of a prototype micropump system is shown in Fig. 2. The micropump we developed is simple structure in the absence of valves, and the fabrication process is accomplished by just stacking organic films or layer on PMMA substrate.

Traveling wave was induced on the bottom surface of the microchannel by applying sinusoidal signals to each lower electrode with the difference of the phase $2\pi/3$, as illustrated in Fig.

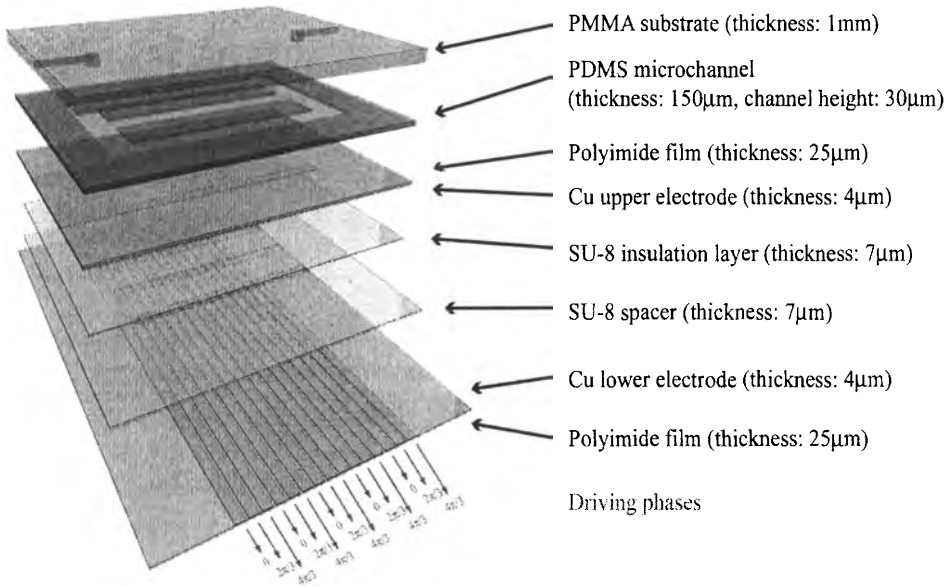

Fig. 1. Exploded view of micropump driven by traveling wave.

3. The fluid can be moved by the peristaltic motion of the channel wall. The microchannel is filled with water in which microbeads with a diameter of 6 μm are spread for the observation of flow condition.

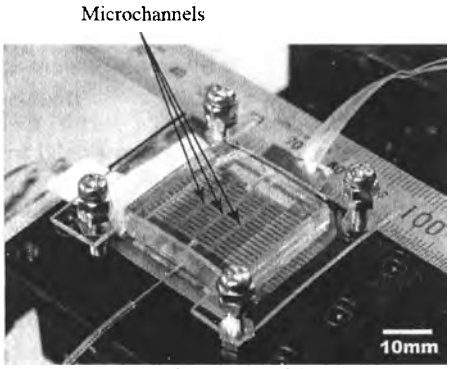

Fig. 2. Photograph of peristaltic micropump driven by electrostatic actuators.

3. Characterization

The deflection of the bottom surface of the channel was measured by the laser Doppler vibrometer. We applied the sinusoidal voltages up to 150 V in amplitude at the frequency of 5.0 kHz to the electrostatic actuators under the microchannel. Although the displacement is not so large as piezoelectric one, we could observe clear deflection of the channel wall. The displacement is proportional to the square of the applied voltage as shown in Fig. 4. The peristaltic motion along the channel wall was successfully generated by the application of the sinusoidal voltages to each lower electrode as shown in Fig. 3. Although continuous flow has not been observed yet, we confirmed active motion of the particles in the fluid by the peristaltic actuation of electrostatic force. These results suggest that the continuous flow can be realized by the optimization of driving signal as well as the structure of the actuators and this system is promising micropumps especially for medical applications.

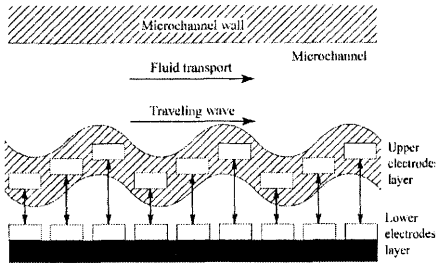

Fig. 3. Fluid transport system using arrayed electrostatic actuators.

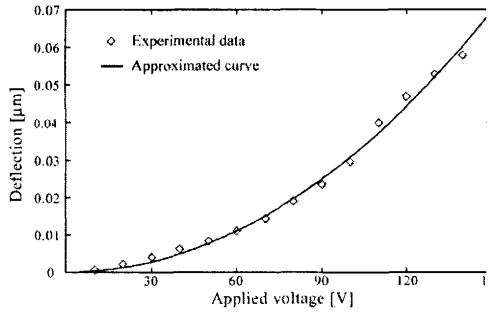

Fig. 4. Deflection of electrostatic actuator diaphragm as a function of applied voltage.

3. Conclusions

The valveless micropump driven by electrostatic actuators has been developed. The micropump was fabricated using flexible layers on PMMA substrate. The bottom of microchannel with electrodes was vibrated by the electrostatic attractors. Traveling wave was induced on the surface of the microchannel by applying sine wave signals with the different phase, and the peristaltic motion of the channel wall transports the fluid. The sign wave signals of 150 V in amplitude were applied at the frequency of 5.0 kHz to the electrostatic actuators under the microchannel filled with the water. The active motion of the particles in the fluid was confirmed by the peristaltic actuation of electrostatic force.

Acknowledgements

This study was supported by Industrial Technology Research Grant Program in '04 from New Energy and Industrial Technology Development Organization (NEDO), Center of Excellence for Research and Education on Complex Functional Mechanical Systems (COE program of the Ministry of Education, Culture, Sports, Science and Technology) and grant-in-aid for Scientific Research (A) (No.14205037 and No. 15201033) from the Ministry of Education, Culture, Sports, Science and Technology, Japan

References

[1] H. T. G. van Lintel, F. C. M. van De Pol and S. Bouwstra, et al., "A Piezoelectric Micropump Based on Micromachining of Silicon", *Sens. Act.*, **15**, 153-167 (1989).
[2] R. Linnemann, P. Woias, C. D. Senfft and J. A. Ditterich, "A Self-priming and Bubble-tolerant Piezoelectric Silicon Micropump for Liquids and Gases", *Proc. IEEE MEMS*, 532-537 (1998).
[3] J. G. Smits, "Piezoelectric Micropump with Three Valves Working Peristaltically", *Sens. Act. A*, **21**, 203-206 (1990).
[4] I. Kanno, S. Kawano, S. Yakushiji and H. Kotera, "Characterization of Piezoelectric Micropump Driven by Traveling Waves", *Proc. μTAS2003*, 997-1000 (2003).

A NOVEL FABRICATION PROCESS FOR 3D-MULTILAYER MICRO MIXERS

Marco Feldmann[1], Andreas Waldschik[1] and Stephanus Büttgenbach[1]
[1]*Institute for Microtechnology, Technical University of Braunschweig, Alte Salzdahlumer Str. 203, 38124 Braunschweig, GERMANY*

Keywords: micro mixer, micro fluidics, PDMS, SU-8, UV-depth lithography

1. Introduction

The integration and miniaturization of biochemical analysis systems (μTAS, lab-on-a-chip) like micro capillary electrophoresis or micro absorption photometry has received considerable attention in research. Particular interest is laid on fully integrated devices with micro fluidic components, like micro valves, micro pumps and micro mixers. However, mixing on a micro scale it is usually difficult to achieve, because viscous effects dominate the flow behavior. On the other hand the laminar nature of the flow in micro channels requires novel approaches to enhance the mixing process. Opposed to one layer micro mixers we developed a novel fabrication process for building 3D-multilayer micro mixers using Epon SU-8 and PDMS. Different passive mixing concepts have been simulated and tested. These concepts are based on the splitting and recombination of streams, using perpendicular inlets to the main channels (injection) and on vortex mixers [1].

2. Mixer concepts

In principle the mixers consists of three layers (see Fig. 1). The first layer contains the lower channels and the second layer the via-interconnects to the third layer, which contains the upper channels. These mixer structures are realized using Epon SU-8 and are covered by two cured PDMS layers. Finally the system and the fluid connectors are sealed with glue and are fixed on a glass substrate (see Fig 2).

3. Simulation

In order to obtain an idea of the optimal geometric dimensions and the achievable mixing ratio, computational fluid dynamics (CFD) simulations were run. In the simulation both fluids were injected simultaneously into the mixer. The CFD results of two different mixers in Fig. 3 and Fig. 4 show an excellent mixing behaviour (green).

4. Fabrication process

The fabrication process for the mixer structures is schematically displayed in Fig. 5. For the sacrificial layer the use of copper showed best performance due to its ease to etch without harming the SU8. Larger parts like the mixers, which need to be taken off completely, can be detached using a thicker Cu film. This thick sacrificial layer (up to a few microns) is deposited by electroplating, providing a broader etch front and reducing diffusion lengths underneath etched structures [2]. After fabrication of the cooper sacrificial layer the first SU-8 layer was deposited by spin coating with a rotating lid spinning tool, bakes on ramped hot plates, exposure and a two solution (GBL and PGMEA) development. Almost vertical sidewalls and aspect ratios of up to 36 were achieved. After this the produced SU-8 structures were electroplated with cooper to fill the lower channels. Then we fabricate a double SU-8 layer on top, which can be realized in two ways. At last the mixer structures were detached by etching the sacrificial layer and finally covered with PDMS. A photograph of a realized mixer is shown in Fig. 6.

5. Results and discussion

The mixers validated in simulation have been build and tested successfully (see Fig. 7 and Fig. 8). Two fluids with different color (blue, yellow) were injected by two micro pumps. As shown in

Fig. 7 a thorough mixing in the vortex mixer could be accomplished. In contrast to Fig. 7 we found, that the mixing ratio in the mixer shown in Fig. 8 is susceptible to interferences caused by the variation between of the flow rates of the micro pumps.

An enhancement of the pumping devices is subject to further investigations. As shown, a powerful means for the fabrication of complex 3D-multilayer micro mixers has been developed and successfully tested.

References

[1] . Böhm, K. Greiner, S. Schlautmann, S. de Vries, A. van den Berg, *Technical Proceedings of Micro Total Analysis Systems, MicroTAS, Monterey, CA,* (2001).

[2] V. Seidemann , J. Rabe , M. Feldmann , S. Büttgenbach, *Microsystem Technologies,* 8(4-5), 348-350 (2002).

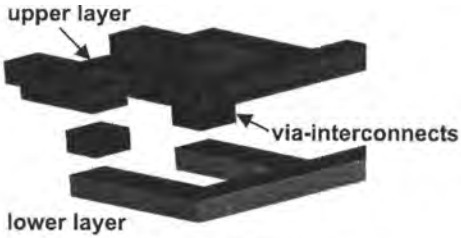

Figure 1. Principle mixer structure

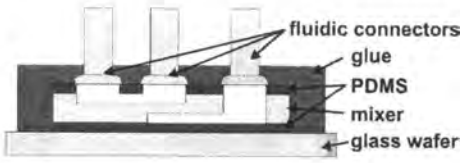

Figure 2. Mixer device

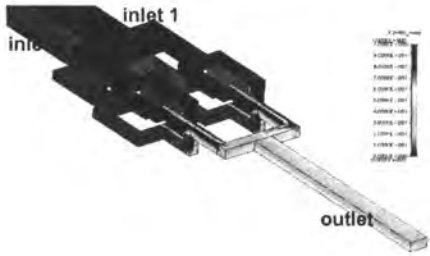

Figure 3. CFD result for an combined splitting and injection

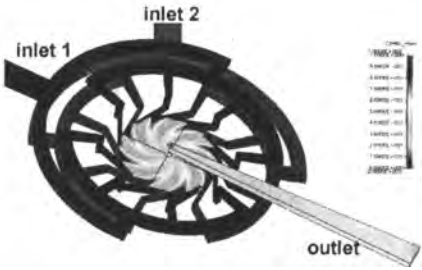

Figure 4. CFD result for an vortex mixer

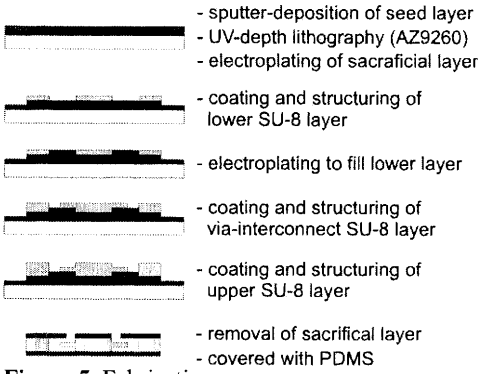

Figure 5. Fabrication process

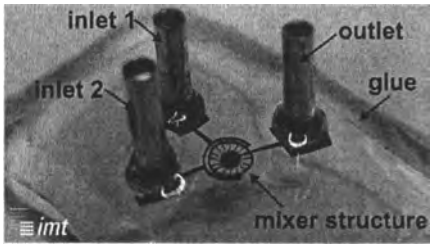

Figure 6. Photograph of a vortex mixer filled with colored water

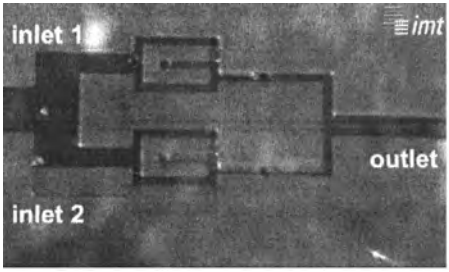

Figure 7. Test of a combined splitting and injection mixer

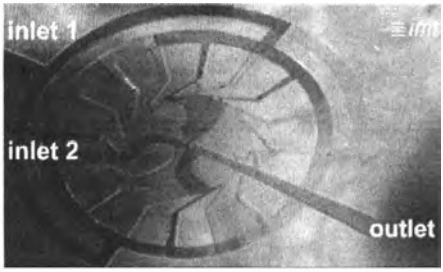

Figure 8. Successful test of an vortex mixer

HIGH PRECISION LOW TEMPERATURE BONDING PROCESS FOR BIOMEMS

Jörg Kentsch, Wolfgang Lutz, Manfried Dürr, Martin Stelzle
NMI - Naturwissenschaftliches und Medizinisches Institut an der Universität Tübingen, Markwiesenstrasse 55, D-72770 Reutlingen, Germany, phone: +49 (0)7121 51530-0, fax: +49 (0)7121 51530-62, e-mail: stelzle@nmi.de

1. Introduction

Today BioMEMS with surfaces functionalized by coating with biological components become more and more important. When working with closed micro channels three problems come up with regard to fabrication technology: (1) how to seal a device without contamination of the channel wall for example with adhesive, (2) how to bond bottom and top substrates without destroying biological components such as antibody coatings by heat as is commonly necessary in anodic bonding and with use of heat curable adhesives, and (3) how to align top and bottom halves with µm precision in order to create for example 3D-electrode arrays for use in dielectrophoresis applications. Also, such a process must lend itself to up-scaling and mass-production.

Keywords: low temperature bonding, adhesive, BioMEMS, microfluidic systems

2. Experimental

These issues were addressed in the development of a novel low temperature bonding process (LTBP) (Figure 1). LTBP has been applied to the fabrication of micro-fluidic devices with embedded electrode arrays. Since micro-electrodes were to be positioned on both faces of the device, most demanding requirements with respect to the precision of alignment had to be fulfilled. In contrast to commonly used high temperature bonding processes such as anodic bonding, our process may also be applied to polymer substrates and in addition allows for very high precision of alignment which is routinely better than ±2µm. The novel bonding process (Fig.1) relies on the precise preparation of an ultrathin film of uv-curable adhesive and its application onto one side of the micro-device.

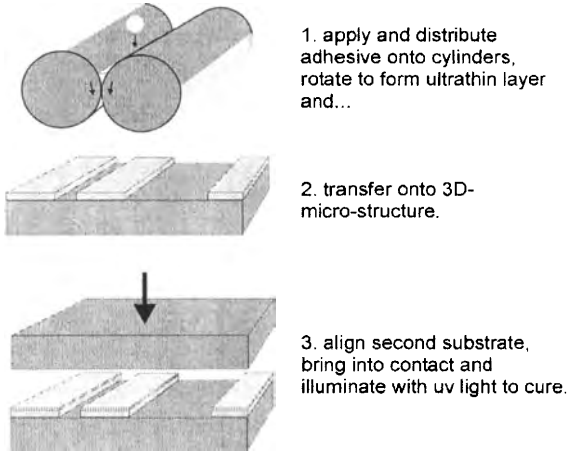

Figure 1. Schematic depiction of LTBP using uv-curable adhesive.

3. Results

This was accomplished using a custom designed tool (Fig.2). By rotating high precision milled cylinders, a layer of adhesive of homogeneous thickness is generated and transferred onto the substrate. Subsequently, both halves of the micro-device are aligned and brought into contact using a modified mask aligner. In-situ exposure employing the illumination source of the mask aligner brings curing of the adhesive to completion.

Bonding of polymers, glass and silicon may be achieved using uv-curable adhesive. Layer thickness may be adjusted by using an adhesive with the appropriate viscosity. Micro-fluidic devices have been fabricated with a channel height of only 5 μm and a thickness of the bonding layer on the order of 1 μm. Even for these shallow channels, contamination of the

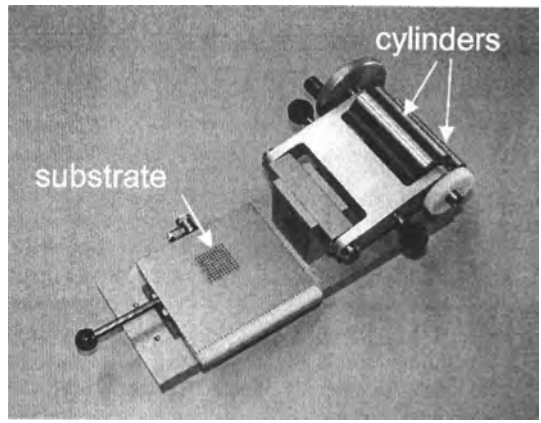

Figure 2. Custom designed tool used for the preparation of ultra-thin homogeneous layers of uv-curable adhesive and their application to micro-devices. High precision milled cylinders rotate against each other thus distributing the adhesive. Final layer thickness depends on viscosity and pressure applied.

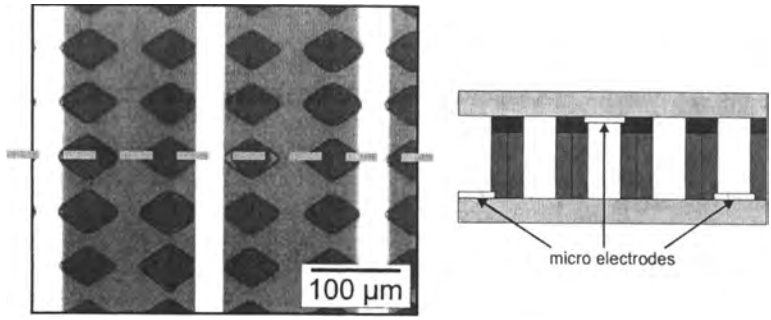

Figure 3. *Left:* Bonding of micro-fluidic devices consisting of glass with micro-electrodes (white bars), micro-patterned SU8 and a glass cover plate with micro-electrodes. The rhombic shaped SU8 columns (side length: 40 μm) together with the adhesive layer result in a total height of the chamber of 16.0μm. Homogeneous thickness of the adhesive layer ensures proper bonding reflected by dark appearance of contact areas while avoiding contamination of channels.
Right: Schematic view of the channel cross section as indicated by the dashed line in the left image.

channels by excess of adhesive may be avoided since layer thickness is very homogeneous. The channel height has been determined by interference measurements [3] with a precision of about 0,25µm.

Fig.3 shows an example of a bonded micro-fluidic system [1], [2] fabricated using LTBP. In this particular example, the micro-channel structure was created (1) using SU8 photoresist on a glass substrate to define micro-channels, (2) application of adhesive to the elevated SU8 structures and (3) bonding the glass/SU8/adhesive structure to another glass substrate serving as cover plate. The dark appearance of the contact areas indicates proper bonding.

4. Conclusion

A novel low temperature bonding process has been developed and applied to the fabrication and high precision bonding of micro-fluidic systems with embedded electrode arrays. This technology avoids problem frequently encountered in BioMEMS fabrication such as contamination of the cover plate with adhesive as well as high temperatures with the related hazard of destruction of biological components. In contrast to anodic bonding, the use of an adhesive bonding scheme allows for a wide range of material combinations to be applied for substrate and cover, respectively. In addition, LTBP should readily be adaptable to large scale production.

References

[1] Dürr, M., et al., *Microdevices for manipulation and accumulation of micro- and nanoparticles by dielectrophoresis,* Electrophoresis, 2003. **24**: p. 722-731.

[2] Dürr, M., et al. *Dielectrophoretic separation and accumulation of (bio)particles in micro-fabricated continous flow systems*, Micro Total Analysis Systems 2001, p.539-540. Monterey, USA: Kluwer Academic Publishers.

[3] H. Günzler, H. Böck, *IR-Spektroskopie, Eine Einführung*, Wiley/VCH, 1983

NOVEL THERMOPLASTIC ELASTOMERS FOR MICROFLUIDIC DEVICE CONSTRUCTION

Arjun P. Sudarsan, Jian Wang, and Victor M. Ugaz
Department of Chemical Engineering, Texas A&M University, College Station, TX 77843, USA

Abstract

We demonstrate the use of thermoplastic elastomer gels as advanced substrates for construction of complex microfluidic systems. These gels are synthesized by combining inexpensive polystyrene–(polyethylene/polybutylene)–polystyrene triblock copolymers with a hydrocarbon oil for which the ethylene/butylene midblocks are selectively miscible. The insoluble styrene endblocks phase separate into localized domains resulting in the formation of an optically transparent, viscoelastic, and biocompatible 3-D network possessing many features typical of soft materials employed as microfluidic device substrates (e.g. poly(dimethylsiloxane) (PDMS)), with the further advantage of melt-processability at temperatures in the vicinity of 100 °C. This desirable combination of properties allows microfluidic devices to be fabricated with unprecedented ease by simply making an impression of the negative relief structures on a heated master mold. The fabrication process can be completed in under 5 minutes, and multiple impressions can be made against different masters to construct geometries incorporating variable-height features, as well as intricate 3-D multilayered structures. Thermal and mechanical properties are tunable over a wide range through proper selection of gel composition.

Keywords: microfluidics, soft lithography, PDMS

1. Introduction

The development of increasingly sophisticated chemical and biochemical assays, combined with the need to incorporate these processes within a compact device footprint suitable for massively parallel operation requires the construction of correspondingly complex microfluidic structures [1,2]. This ongoing drive toward increased device complexity requires corresponding advances in fabrication materials and technologies. For example, although a number of multilayer PDMS-based systems have been successfully constructed, the resulting fluidic networks are effectively 2-dimensional owing to the planar nature of the fabrication process. It is possible in principle to employ an arbitrary number of layers, however the entire device structure must be assembled at once due to the irreversibility associated with the curing process. This irreversibility can be advantageous in terms of ensuring excellent mechanical stability, however it also imposes limitations because the molded structures cannot be further modified after curing. Consequently, there is no straightforward process to fabricate structures incorporating features of variable height because only a single impression from a single master can be used. Finally, the range of viscoelastic properties available for design of fluidic components that operate by inducing deformations in the substrate material (e.g. valves, pumps) is somewhat limited.

2. Theory

Novel thermoplastic elastomer gel substrates offer the capability to provide a greatly enhanced level of flexibility in microfluidic device design and construction. These gels are easily synthesized using a combination of inexpensive polystyrene–(polyethylene/polybutylene)–polystyrene (SEBS) triblock copolymers in hydrocarbon oils for which the ethylene/butylene midblocks are selectively miscible. The thermodynamic incompatibility between blocks induces microphase separation and self assembly of the insoluble polystyrene endblocks into distinct domains with characteristic size scales on the order of 10-20 nm [3,4]. The soluble midblocks emanating from these nanodomains penetrate into the solvent creating arrays of loops (beginning and terminating within a single

nanodomain) and bridges (joining adjacent nanodomains) resulting in the formation of a 3-D viscoelastic gel network in which the polystyrene domains act as physical crosslink junctions. Like PDMS, this gel network is optically transparent, viscoelastic, and biocompatible, but also possesses the further advantage of melt-processability at temperatures in the vicinity of 100 °C.

3. Experimental

A series of thermoplastic elastomer gels were synthesized by combining commercially available SEBS copolymer resin (Kraton® G series) in mineral oil. The reisn and mineral oil were mixed and placed under vacuum overnight at room temperature in order to allow the oil to evenly wet the resin surface. The mixture was then heated to 120-170 °C (higher temperatures are required with increasing copolymer fraction) under vacuum for 2–4 hours to allow the resin and oil to intermix and to remove any residual air bubbles. Finally, the mixture was cooled to room temperature and the solidified gel was cut into smaller pieces used for molding devices. Gel compositions ranging from 10 to 55 wt% copolymer were studied.

4. Results and discussion

We investigated thermal transitions associated with these SEBS-mineral oil gels using small amplitude oscillatory shear experiments (Fig 1). A measure of the transition to liquid-like behavior can be inferred from the temperature T^* at which the value of the loss modulus G'' exceeds that of the storage modulus G'. The range of gel compositions studied here allow the location of this transition to be varied over a range of approximately 50 °C. Moreover, the room temperature (plateau) value of the elastic modulus can be varied over an order of magnitude.

Fabrication of microfluidic devices is accomplished by placing a slab of elastomer on top of a master mold that has been preheated to 120 °C on a hot plate. Within seconds the elastomer begins to soften, after which a glass plate is placed on top of the slab and gentle pressure is applied by hand to ensure complete contact with the structures on the mold. After cooling and release, the solidified gel incorporates the shape of the structures on the master (Fig 2). Strong uniform bonds can be easily achieved, either with a glass or elastomer surfaces, by briefly heating the material to a temperature just below its softening point either on a hot plate or using a handheld heat gun. The entire fabrication process can be completed in about 5 minutes.

We have demonstrated the suitability of these elastomers as substrates for microfluidic applications by constructing devices for DNA electrophoresis (Fig 3) and diffusive transport studies [5]. We are also able to easily assemble a variety of complex multilayered structures in only a few minutes (Fig 2). Individual layers are repositionable, thereby allowing precise alignment to be achieved prior to thermal bonding. More complex 3-D structures can be fabricated by direct casting, and interfaces with external fluidic supply lines can be readily sealed by locally heating the gel to melt it at the point where the lines are inserted into the substrate. Multiple impressions can be made against different masters to easily construct geometries incorporating variable-height features (Fig 4). This degree of versatility and fabrication ease, combined with their inherently inexpensive nature, make thermoplastic elastomer gels ideal substrates for many microfluidic applications.

References

[1] T. Thorsen, S.J. Maerkl, and S.R. Quake, *Science,* **298**, 580-584 (2002).
[2] S. Sia and G.M. Whitesides, *Electrophoresis,* **24**, 3563-3576 (2003).
[3] J.H. Laurer, J.F. Mulling, S.A. Khan, R.J. Spontak, and R. Bukovnik, *J. Polym. Sci.: Part B: Polym. Phys.,* **36**, 2379-2391 (1998).
[4] R. Kleppinger, N. Mischenko, H.L. Reynaers, and M.H.J. Koch, *J. Polym. Sci.: Part B: Polym. Phys.,* **37**, 1833-1840 (1999).
[5] A.P. Sudarsan and V.M. Ugaz, *Anal. Chem.,* **76**, 3229-3235 (2004).

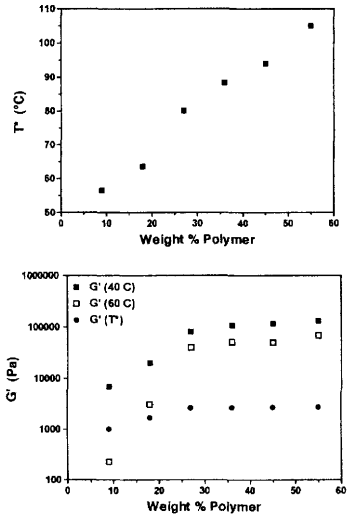

Figure 1. Variation of melt transition temperature (top) and plateau elastic modulus (bottom) with gel composition.

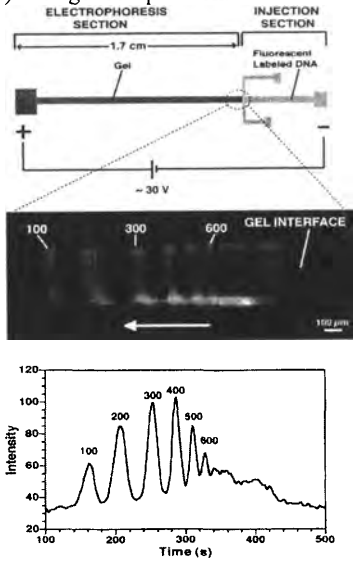

Figure 3. DNA gel electrophoresis device constructed using thermoplastic elastomer. An image of the fluorescent bands and electropherogram obtained 2 mm downstream from the gel interface are shown (E = 15 V/cm).

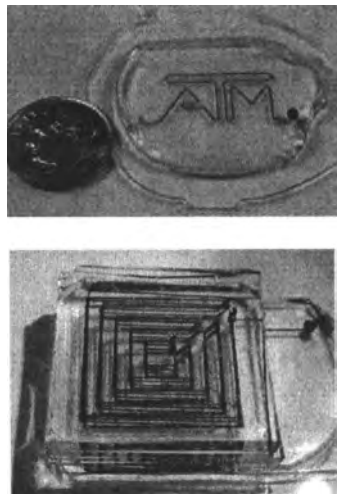

Figure 2. Planar (top) and interconnected multilayer (bottom) microfluidic channels constructed using elastomer gels (400 x 30 μm cross-section).

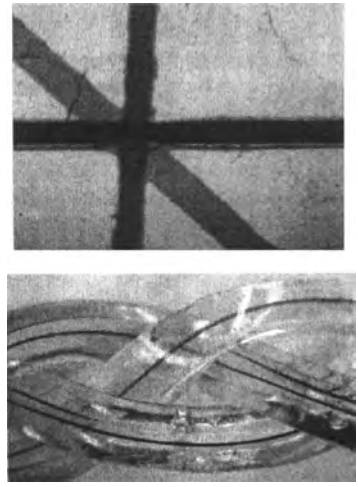

Figure 4. (Top) Intersecting fluidic channels with 3 different depths in a single elastomer substrate. Horizontal: 300 x 120 μm, vertical: 200 x 60 μm, diagonal: 400 x 30 μm cross-sections. (Bottom) Braided network of intertwined elastomer channels.

ELECTROSTATIC SHAKING AND CONVEYANCE OF CATALYTIC PARTICLES IN MICRO SPACES

Koichi Suzumori[1], Takefumi Kanda[1], Takashi Nagata[1], Akinori Muto[2], and Yusaku Sakata[2]
[1] *Dept. of Systems Engineering, Okayama University, Tsushima-naka, Okayama 700-8530 Japan*
[2] *Dept. of Applied Chemistry, Okayama University, Tsushima-naka, Okayama 700-8530 Japan*

Abstract

This paper reports a new electrostatic handling method of catalytic particles in micro spaces. It causes shaking of the particles in a micro chamber to realize uniform mixing of chemical materials and acceleration of reaction. It also causes conveyance of the particles along micro channels or pipes. The actuator mechanism is very simple and suitable to be fabricated through MEMS process.

Keywords: micro reactor, active catalyst, electrostatic actuator, micro stirrer

1. Introduction

Uniform mixing and acceleration of chemical reaction in micro chambers are an essential process for micro reactors and micro TAS. However, it is difficult to fabricate many tiny stirrers on a reactor chip. This paper shows a new method promoting high-efficient chemical reaction in micro chambers; newly developed carbon-base and zeolite-base catalytic particles are introduced into chamber and driven electrostatically to travel rapidly in chamber, stirring chemicals and accelerating reaction.

In addition, this system works to exchange catalytic particles. Deactivated catalytic particles in chamber are easy to be flushed away with no voltage applied to the electrodes. After flushing, virgin catalytic particles are introduced with gas from the port and they can be kept easily in the chamber by applying voltage. Conveyance of chemical materials along micro channels or pipes is also realized.

2. Electrostatic driving mechanism

Figure 1 shows a typical simple model of a micro reactor proposed in this paper. This model has two inlet ports, an outlet port, a micro chamber, fluidic channels and two thin film electrodes. It can be used for methanol synthesis for example; H_2 and CO_2 gasses are supplied through each inlet port. Applying voltage to the electrodes keeps the catalytic particles inside the chamber and drives them to mix the gasses uniformly and to accelerate methanol synthesis, resulting in high-efficient chemical reaction.

We applied two catalytic particles, zeolite particle and nickel-carbon composite particles ranging in size from 50 μm to 1 mm in diameter. Figure 2 shows nickel-carbon particles of 250μm in diameter. These particles work as catalysts themselves and can contain other catalytic chemicals on their inner surfaces, making this system widely applicable for various types of chemical reactions.

We have developed two driving voltage patterns applied to the electrodes; a DC drive and an AC drive. The DC drive is applicable for conductive particles, while the AC drive is applicable both for nonconductive and conductive particles. Figure 3 (a) shows a driving mechanism of the DC drive: a negatively-charged particle is drawn to the positive electrode as shown in (1), the particle releases electrons and is charged positively as shown in (2) to (3), then the positively-charged particle starts to move to the negative electrode as shown in (4), and the particle is charged negatively again as shown in (5) to move to the positive electrode as shown in (1). This drive needs no electrical switching and is very simple. Frequency of particle motion depends on electrical characteristics of particle and on viscous resistance of vapor/fluid in the chamber.

The AC drive mechanism is shown in Fig. 3 (b). Applying electrostatic field causes polarization in a particle. Phase difference between alternating electrostatic field and polarization results in

oscillation of the particle. Shaking frequency depends mainly on AC drive frequency.

3. Experiments

Figure 4 shows an example of catalytic particles traveling in a micro chamber. The upper photograph shows the particles at rest. The lower photograph, which was taken with the exposure time of 100 msec shows the particle traveling rapidly in the chamber.

The chamber is formed by two cupper walls and two glass plates. The chamber is 3 mm in width. We have tried three particles in this chamber; nickel-carbon composite particles of 250μm and 500 μm in diameter, and zeolite particles of 500μm in diameter. Applying DC or AC voltage between two cupper walls we can drive the nickel-carbon composite particles in the chamber. We also succeed at driving the zeolite particles by applying AC voltage. Applied voltage between the cupper walls is adjustable from 0 to 3.0 kV.

It was found that (1) the DC drive method is applicable for nickel-carbon particles of 250 μm and 500 μm, and the AC drive is applicable both for nickel-carbon particles and zeolite particles, (2) the particles can be driven by applying minimum electrostatic fields of $1x10^5$ V/m, and (3) frequency of particle motion is up to 10 Hz.

Figures 5 and 6 show the glass tube models: the model shown in Fig.5 has two aluminum thin films sputtered on the outer surface of the tube to realize shaking the particles in tubes. The model shown in Fig. 6 has the strip electrodes of sputtered aluminum film to convey particles rapidly in desired direction by applying voltage to each electrode sequentially. This system works to exchange catalytic particles. The glass tube is 2 mm in inner diameter.

The glass tube models work successfully. Both nickel-carbon particles and zeolite particles are easily driven by applying 1 to 3 kV AC voltage.

4. Conclusions

A new method realizing uniform mixing and acceleration of chemical reaction in a micro chamber is proposed. Experiments using two prototypes show that the proposed method makes the catalytic particles traveling rapidly in micro chamber and moving in pipes. It is found that electrostatic fields of $1x10^5$ V/m is necessary and driving frequency is about 10 Hz in air.

We believe that this method can be applied to various gas phase chemical reactions in micro reactors and micro TAS. We are now making experiments to determine reaction efficiency.

Acknowledgements

This work was supported by the Cooperation of Innovative Technology and Advanced Research in Evolutional Area (CITY AREA) of the Ministry of Education, Culture, Sports, Science and Technology, Japan.

Reference

[1] Takashi Nagata, Koichi Suzumori, Takefumi Kanda, Akinori Muto, and Yusaku Sakata, Electrostatic Shaking of Catalytic Particles in Micro Chamber, The Second International Workshop on Micro Chemical Plants, Awaji, Japan, February 2004.

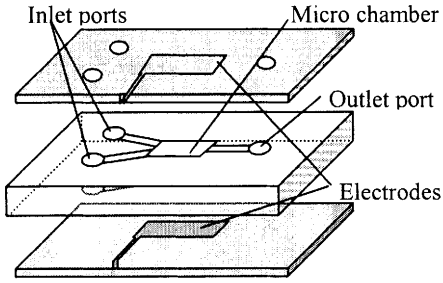

Figure 1. Schematic of a typical model of a micro reactor with shaking catalyst system

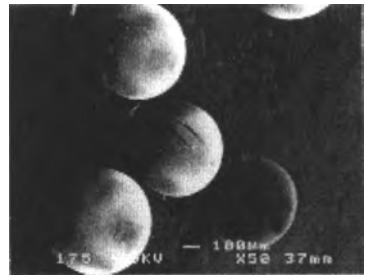

Figure 2. An example of catalytic particles (nickel-carbon composite, 250 μm in diameter)

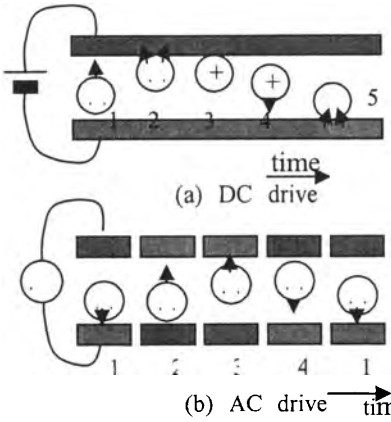

Figure 3. Driving mechanism of shaking particles shaking

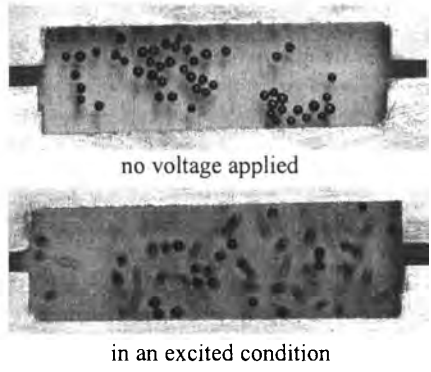

Figure 4. Motions of catalytic particles, shaking in a micro chamber (Exposure time is 100 msec.)

Figure 5. A glass tube mode (shaking type)

Figure 6. A glass tube model (conveyance type)